Published in final edited form as:
Vet J. 2013 November ; 198(2): . doi:10.1016/j.tvjl.2013.08.015.

Canine intracranial gliomas: Relationship between magnetic resonance imaging criteria and tumor type and grade

R.T. Bentley[a,*], **C.P. Ober**[b], **K.L. Anderson**[b,1], **D.A. Feeney**[b,1], **J.F. Naughton**[a,1], **J.R. Ohlfest**[c,2], **M.G. O'Sullivan**[d], **M.A. Miller**[e], **P.D. Constable**[a], and **G.E. Pluhar**[b]

[a]Department of Veterinary Clinical Sciences, Purdue University, West Lafayette, IN 47907, USA

[b]Department of Veterinary Clinical Sciences, University of Minnesota, Saint Paul, MN 55108, USA

[c]Masonic Cancer Center, University of Minnesota, Minneapolis, MN 55455, USA

[d]Department of Veterinary Population Medicine, University of Minnesota, Saint Paul, MN 55108, USA

[e]Department of Comparative Pathobiology, Purdue University, West Lafayette, IN 47907, USA

Abstract

Limited information is available to assist in the ante-mortem prediction of tumor type and grade for dogs with primary brain tumors. The objective of the current study was to identify magnetic resonance imaging (MRI) criteria related to the histopathological type and grade of gliomas in dogs. A convenience sample utilizing client-owned dogs (*n*=31) with gliomas was used. Medical records of dogs with intracranial lesions admitted to two veterinary referral hospitals were reviewed and cases with a complete brain MRI and definitive histopathological diagnosis were retrieved for analysis. Each MRI was independently interpreted by five investigators who were provided with standardized grading instructions and remained blinded to the histopathological diagnosis.

Mild to no contrast enhancement, an absence of cystic structures (single or multiple), and a tumor location other than the thalamo-capsular region were independently associated with grade II tumors compared to higher grade tumors. In comparison to oligodendrogliomas, astrocytomas were independently associated with the presence of moderate to extensive peri-tumoral edema, a lack of ventricular distortion, and an isointense or hyperintense T1W-signal. When clinical and MRI features indicate that a glioma is most likely, certain MRI criteria can be used to inform the level of suspicion for low tumor grade, particularly poor contrast enhancement. Information obtained from the MRI of such dogs can also assist in predicting an astrocytoma or an oligodendroglioma, but no single imaging characteristic allows for a particular tumor type to be ruled out.

[*]Corresponding author. Tel.: +1 765 494 1107. rbentley@purdue.edu (R.T. Bentley).
[1]These authors contributed equally to this work.
[2]Manuscript submitted posthumously in this author's name.

Conflict of interest statement
None of the authors of this paper has a financial or personal relationship with other people or organizations that could inappropriately influence or bias the content of the paper.

Keywords

Astrocytoma; Oligodendroglioma; Glioma; Dog; Brain; Imaging

Introduction

The magnetic resonance imaging (MRI) features of gliomas and other intra-axial primary brain tumors in dogs have been described (Cervera et al., 2011; Kraft et al., 1990, 1997; Lipsitz et al., 2003; Ródenas et al., 2011; Snyder et al., 2006; Wolff et al., 2012), but only recently have associations between the MRI appearance and the tumor type or the tumor grade been studied (Young et al., 2011). Typical canine intracranial gliomas are intra-axial, T1W- iso- to hypo-intense, T2W- iso- to hyper-intense mass lesions with varying perilesional edema and contrast enhancement (Kraft et al., 1997; Ródenas et al., 2011; Snyder et al., 2006; Young et al., 2011).

Some MRI features have been related to type and grade of canine glioma. The presence of contrast enhancement was significantly associated with tumor grade (Young et al., 2011). Cysts and areas of necrosis have not been significantly related to grade, but are common in higher grade tumors (Lipsitz et al., 2003; Young et al., 2011). Differentiation between areas of necrosis, and single and multiple cystic structures has not been previously studied in glioma in dogs; however, a technique for describing either a single cyst or at least one intratumoral accumulation of fluid (ITF) has been reported for meningioma (Sturges et al., 2008). Regarding tumor type, surface contact was reported to be significantly more common with oligodendrogliomas (Young et al., 2011), but distortion of ventricles has not yet been reported to be significantly more common (Kraft et al., 1997; Ródenas et al., 2011; Young et al., 2011).

For glioma in humans, various MRI features can be used to predict tumor type and grade (Dean et al., 1990; Jenkinson et al., 2007; Provenzale et al., 2006; Watanabe et al., 1992). Accordingly, using MRI to predict the type and grade of canine tumors may be possible. As surgery is expensive and invasive, and canine gliomas are routinely treated with modalities such as radiation therapy without histopathological confirmation (Bley et al., 2005; Brearley et al., 1999), information that can be used to better predict tumor type and grade could be useful. Canine gliomas are not routinely managed based on a division between low grade glioma (grades I and II) and high grade gliomas (grades III and IV), although this is standard in human medicine (Watanabe et al., 1992; Dean et al., 1990; Cavaliere et al., 2005). Higher grade tumors can be suspected based on imaging characteristics such as irregular or ring-like contrast enhancement or signal intensity in humans, and this can be used to guide therapy (Watanabe et al., 1992; Forbes et al., 2011; Rao et al., 2013).

Based primarily on a review of the MRI literature relating to canine gliomas (Cervera et al., 2011; Kraft et al., 1990, 1997; Lipsitz et al., 2003; Polizopoulou et al., 2004; Snyder et al., 2006; Sturges et al., 2008) and a pilot study (Bentley et al., 2010), and secondarily to studies of human gliomas (Dean et al., 1990; Jenkinson et al., 2007; Provenzale et al., 2006), we hypothesized that increasing tumor grade is related to increasing degree of contrast enhancement, the formation of single cysts or multiple ITFs, and T2*-weighted gradient echo (GRE) signal voids. Regarding tumor type, we hypothesized that ventricular distortion is more common with oligodendrogliomas than astrocytomas.

Materials and methods

Animals and tumors

The medical records of dogs admitted to two veterinary teaching hospitals (Purdue University, University of Minnesota) between 30 July 2007 and 10 October 2010 were reviewed and cases for which histology confirmed intracranial structural lesions, and for which a complete MRI of the brain was performed before histological diagnosis, were retained for analysis. Only dogs with a histopathological diagnosis of glioma were included as cases. The MRIs of 25 dogs with structural intracranial lesions other than gliomas were also retained as distractors. These were provided to the investigators reading the MRIs mixed with the MRIs of gliomas in a blinded fashion; the results were not used in the statistical analyses.

One veterinary pathologist (GOS, MAM) at each institution provided a histological diagnosis using previously described criteria (Koestner et al., 1999; Louis et al., 2007). Hematoxylin and eosin (H&E)-stained sections and glial fibrillary acidic protein (GFAP) immunohistochemistry were available for all cases. Grading was performed according to the 2007 WHO classification of human tumors (Louis et al., 2007) and a numerical grade was then applied to each tumor as described for canine gliomas (Young et al., 2011).

Evaluation of magnetic resonance imaging

The MRIs were independently evaluated by five investigators, including Board-certified radiologists (CPO, KLA, DAF, JFN) and a Board-certified neurologist (RTB). Each investigator was masked to the histopathological diagnosis and provided standardized grading instructions. The MRIs were graded on 18 criteria similar to those used in previous studies (Kraft et al., 1997; Lipsitz et al., 2003; Ródenas et al., 2011; Snyder et al., 2006) and further developed in our pilot study (Bentley et al., 2010). For 17 criteria, investigators chose one option from a list of 2–5 options (Table 1). Investigators were instructed to provide a free-response description of the anatomic location of the tumor for the final criterion. Following data collection, tumors were grouped into four locations; Location 1 (frontal or fronto-olfactory); Location 2 (parietal lobe or adjacent corpus callosum, temporal lobe); Location 3 (diencephalic or any portion of the internal capsule); and Location 4 (caudal fossa). Both cortical lesions and subcortical lesions were included within the frontal, parietal and temporal classifications (Locations 1 or 2), respectively. Tumors were ascribed to multiple locations as appropriate.

Specific instructions were supplied to the investigators for some MRI criteria. If margins were indistinct, they were considered poorly defined; clear tumor margins were divided into smooth and irregular margins. For mass effect, all features were considered, including ventricular distortion and brain herniations. Both T1W- and T2W-intensities were considered with respect to normal grey matter and the signal from the largest fraction of the tumor was recorded. For T1W- and T2W-homogeneity, tumors were only considered homogenous if nearly all the tumor displayed matching signal intensity. Peri-tumoral edema restricted to one brain division was given an objective grade, while edema of an entire cerebral hemisphere or of multiple brain divisions was graded as extensive. For contrast enhancement severity, only the most severely enhancing portion of the tumor was considered. For brain herniations, the most severe herniation present was selected.

Statistical analysis

Inter-observer agreement for each MRI criterion was assessed by calculating the value for linearly weighted kappa (κ) for each pair of investigators, providing a total of 10 (κ) values for each criterion (PROC FREQ, SAS 9.2, SAS Institute). The overall level of agreement for

each criterion was summarized by the median kappa value for the 10 investigator pairs; values of 0.81–1.00 were considered to indicate excellent agreement; 0.61–0.80, good agreement; 0.41–0.60, moderate agreement; 0.21–0.40, fair agreement; 0.01–0.20, poor agreement, and 0.00, chance agreement (Landis and Koch, 1977), as previously applied to canine brain MRI studies (Wolff et al., 2012).

Statistical analysis of the relationship between the MRI criteria and the tumor type and grade was performed in two stages, a preliminary univariate analysis and a final multivariate analysis. For the preliminary univariate analysis, contingency tables were developed. Grade II tumors were compared to grade III and IV tumors for consistency with prior studies (Young et al., 2011), thus dividing the cases into low-grade and high-grade glioma as in studies of human tumors (Rao et al., 2013). Separately, astrocytomas were compared to oligodendrogliomas. Each contingency table was analyzed using a Fisher's exact test (PROC FREQ, SAS 9.2, SAS Institute) and $P < 0.01$ was considered significant, because of the high number of putative variables examined. Patterns of contrast enhancement were further investigated post hoc by determining associations with no contrast enhancement and with partial or complete ring enhancement.

For multivariate analysis, forward stepwise logistic regression (PROC LOGIST, SAS 9.2, SAS Institute) was used. Again, grade II tumors were compared to grades III and IV and astrocytomas were compared to oligodendrogliomas. A P value to enter of < 0.20 and to remain of < 0.05 was used. Investigators were entered as dummy variables and the final logistic regression model fit was evaluated using the Hosmer-Lemeshow goodness-of-fit test.

Results

Cases

Thirty-one cases of glioma were evaluated, providing 155 MRI interpretations by five investigators. The five investigators additionally evaluated the MRIs of 25 distractors which were not included in the statistical analysis. The 31 cases included 17 astrocytomas and 14 oligodendrogliomas, composed of grade II to IV tumors (Table 2). One brainstem oligodendroglioma exhibited diffuse infiltration of neoplastic GFAP negative glial cells in the prosencephalon, consistent with gliomatosis cerebri. Fifteen astrocytomas and 10 oligodendrogliomas were diagnosed by surgical biopsy. The histopathologically-confirmed distractors not used in statistical analysis were meningiomas ($n = 11$), other extra-axial tumors ($n = 4$), meningoencephalitis ($n = 5$), primitive neuroectodermal tumors (PNET; $n = 3$), benign intraparenchymal hemorrhage ($n = 1$) and radiation therapy-induced necrosis following treatment of a nasal tumor ($n = 1$).

Magnetic resonance imaging

Time between MRI and histological diagnosis was variable but was < 47 days, except for one case that underwent surgery 140 days after MRI. Some MRI studies were performed at other institutions leading to variability in MRI sequences. Images were acquired in transverse, sagittal and dorsal planes. Field strength for both cases and distractors was 0.2–0.5T ($n = 3$), 1.0T ($n = 13$), 1.5T ($n = 29$) or 3.0T ($n = 11$); all studies included pre-contrast T1W, T2W and post-contrast T1W images. The intravenous gadolinium-based contrast agent administered varied according to institution, but was either 0.11 mL/kg of gadodiamide (Omniscan, 287 mg/mL, GE Healthcare) or 0.2 mL/kg of gadopentetate dimeglumine (Magnevist, 469 mg/mL, Bayer Healthcare Pharmaceuticals) for most cases. T2-weighted Fluid Attenuation Inversion Recovery (FLAIR) images were acquired on 30/31 cases and T2*-weighted GRE images were attained on 24.

Inter-observer agreement on evaluation of magnetic resonance imaging

The median inter-observer agreement (weighted κ statistic) for the 31 cases (Table 3) demonstrated an overall median κ value of 0.50, indicating that general agreement was moderate. Only those MRI criteria divided into two categories for inter-observer agreement analysis achieved excellent agreement: intra- or extra-axial origin, Locations 2 and 4, gradient echo signal voids and T1W-intensity.

Two MRI criteria were not evaluated any further: leptomeningeal involvement, as this resulted in poor inter-observer agreement ($\kappa = 0.02$), and the tumor origin, as this was almost universally recorded as intra-axial (153/155 observations).

Tumor grade

Following inter-observer agreement analysis, selected MRI criteria were collapsed into a smaller number of options for meaningful statistical analysis, consistent with previous studies as follows. Degree of contrast enhancement (none or mild vs. moderate or severe), T1W-signal intensity (hypointense vs. isointense or hyperintense), T2W-signal intensity (hyperintense vs. isointense or hypointense), peri-tumoral edema (none or mild vs. moderate, severe or extensive) and shape (spherical or ovoid vs. all others). The presence of any degree of ventricular distortion was compared to the absence of distortion in order to address our tumor type hypothesis.

In the preliminary univariate analysis, associations ($P < 0.01$) were found between tumor grade and eight MRI criteria: contrast enhancement pattern (all patterns), no contrast enhancement, partial or complete ring enhancement, moderate or severe contrast enhancement, gradient echo signal voids, T2W-heterogeneity, a single cyst and ventricular distortion (Table 4). Ring enhancement was more often a complete ring (31% of all tumors) rather than a partial ring (16%), while a patchy (non-uniform) pattern of contrast enhancement was seen in around one quarter of tumors of all grades. Focal enhancement of a part of the tumor and uniform enhancement of the entire tumor were rare, each being seen in < 10% of tumors of all grades; the remaining tumors showed no contrast enhancement.

The final multivariate logistic regression indicated four MRI criteria independently associated with being less common in grade II tumors ($P < 0.05$). Single cysts (odds ratio (OR), 0.12 (95% confidence limits [CL], 0.04–0.37); $P = 0.0003$) and multiple ITFs (OR, 0.18 [95% CL, 0.06–0.54]; $P = 0.0023$) were less common in grade II tumors. Moderate or severe contrast enhancement was less common (OR, 0.18 [95% CL, 0.07–0.52]; $P = 0.0014$). Finally, some or all of the tumor situated in Location 3 (the diencephalon and any portion of the internal capsule, Figs. 1–3) was also less common (OR, 0.19 [95% CL, 0.04–0.94]; $P = 0.042$). The Hosmer-Lemeshow goodness-of-fit test indicated a good fit of the final logistic regression model ($P = 0.67$).

Tumor type

In the preliminary univariate analysis, there were two significant ($P < 0.01$) associations with astrocytomas in comparison to oligodendrogliomas (Table 7), T1W-hypointensity and ventricular distortion. At least mild perilesional edema was recorded in 87% of the 155 MRI interpretations, but with no significant difference ($P = 0.012$) between astrocytomas and oligodendrogliomas in the occurrence of moderate to extensive peritumoral edema in the univariate analysis.

Final multivariate logistic regression indicated that astrocytomas were significantly ($P < 0.05$) associated with the presence of moderate to extensive peri-tumoral edema (Fig. 4) (OR, 3.17 [95% CL, 1.47–6.86]; $P = 0.0033$), a lack of ventricular distortion (OR, 0.29

[95% CL, 0.12–0.67]; $P = 0.0036$), and an isointense to hyperintense T1W-signal (OR of T1W-hypointensity 0.25 [95% CL, 0.08–0.73]; $P = 0.011$). The Hosmer-Lemeshow Goodness-of-Fit test indicated a good fit of the final logistic regression model ($P = 0.96$).

Discussion

Our multivariate analyses suggest that for canine intracranial gliomas, MRI can be used to predict a higher likelihood of a grade II tumor, utilizing no to mild contrast enhancement, the absence of cystic regions, and a location superficial to the diencephalon and any part of the internal capsule. Astrocytomas can be less well distinguished from oligodendrogliomas using a lack of ventricular distortion and the presence of moderate to extensive edema; T1W-hypointensity may or may not be useful in light of previous studies. We confirmed our hypotheses regarding contrast enhancement, cystic structures and ventricular distortion, but not T2*-weighted GRE signal voids.

Our findings can only be used with respect to glioma as one of the differential diagnoses for canine intra-axial lesions. When provided with clinical data and MRI, investigators can suspect intracranial glioma with high sensitivity (91%) and specificity (94%) in dogs (Wolff et al., 2012), but other tumors including PNET or lymphoma (Ródenas et al., 2011; Snyder et al., 2006), and lesions such as cerebrovascular accident and inflammatory disease (Cervera et al., 2011; Wolff et al., 2012) must still be retained in the differential diagnosis.

Our study should be interpreted in light of one similar study (Young et al., 2011), which was published after our data collection, resulting in differing methodologies. We used comparable methodology to assess the importance of contrast enhancement and also found significantly less enhancement in grade II tumors. However, this previous study compared no enhancement to any enhancement in contrast to our multivariate analysis indicating that either a lack of enhancement or mild enhancement are more common in grade II tumors. The repeatability of the significance of contrast enhancement in the prediction of tumor grade indicates it may be our most robust conclusions. We also used similar methodologies to assess cystic regions, but generated conflicting results regarding the relationship with grade, although the previous study by Young et al. (2011) did not use T2W FLAIR images. That study also did not analyze the significance of deep, thalamo-capsular tumors, whereas it found a significant relationship between oligodendrogliomas and contact with the brain surface, a criterion that we unfortunately did not examine in our study. Finally, Young et al. (2011) did not examine ventricular distortion, but rather tumor contact with the ventricles, which may be a major reason why our findings appear to differ with respect to the significance of interactions with ventricles.

A lack of enhancement was seen in about half of the grade II tumors in our study, and most grade II tumors in the Young et al. (2011) study. Meanwhile, all grade IV tumors showed at least some enhancement in our study, as did a total of 12/13 glioblastomas in previous reports (Giri et al., 2011; Lipsitz et al., 2003; Snyder et al., 2006; Young et al., 2011). Contrast enhancement is correlated to grade in human glioma, with central non-enhancing portions being typical for glioblastoma (Jenkinson et al., 2007). Overall, studies in dogs appear to support that contrast enhancement is one of the most important means of classifying gliomas, and that in particular a complete lack of contrast enhancement is more common for grade II tumors (Young et al., 2011) and uncommon for glioblastoma.

Cystic regions or necrosis are typical for canine glioblastoma (Lipsitz et al., 2003) and correlate to glioma grade in humans (Dean et al., 1990; Watanabe et al., 1992). Our study conflicted with the Young et al. (2011) study regarding their signficance in the prediction of grade, and it should be noted that cystic regions (either single cysts or multiple ITFs)

occurred in about one third of the low grade tumors in our study. Consequently, cystic regions should never be used to rule out low grade tumors. A T2-weighted FLAIR sequence should ideally be performed in MRIs of dogs with intra-axial brain lesions in order to better characterize fluid accumulations and differentiate cavitary lesions from edema or other parenchymal high signal.

We did not hypothesize that tumors in a deeper location involving the diencephalon or the internal capsule (Location 3) were associated with high tumor grade, although in one publication four of five canine glioblastomas involved the thalamus, internal capsule, or brainstem (Lipsitz et al., 2003). As surface contact is significantly more common with oligodendrogliomas than astrocytomas (Young et al., 2011), and astrocytomas are eight times more likely to involve the diencephalon than other brain tumors (Snyder et al., 2006), tumor type, grade and location may be interlinked, but the precise relationships need further definition.

Oligodendrogliomas distorted ventricles more commonly than astrocytomas as hypothesized. Around 90% of oligodendrogliomas and astrocytomas contact ventricles in dogs (Young et al., 2011), but oligodendrogliomas often occur particularly proximate to the lateral ventricle (Kraft et al., 1997; Ródenas et al., 2011; Snyder et al., 2006), which may explain why they are more likely to actually distort ventricles, rather than merely make contact. In fact, our results indicate that even distortion is common for both astrocytomas and oligodendrogliomas, but that an absence of ventricular distortion increases the suspicion of astrocytoma.

Our study and the study of Young et al. (2011) found that the majority of gliomas display at least some peritumoral edema. Different methodologies were used, such that the presence of perilesional T2W-hyperintensity of any degree was not statistically significantly different between astrocytomas and oligodendrogliomas in the study of Young et al. (2011), but moderate to extensive edema was more common in astrocytomas in our study. In another study, peritumoral edema was not detected on MRI of 7/19 oligodendrogliomas, but was absent around just 1/9 astrocytomas (Dickinson et al., 2008), and human oligodendrogliomas also typically display absent to mild peritumoral edema (Engelhard et al., 2003). However, any degree of edema may be seen with any type of glioma or other tumor.

Due to the retrospective nature of our study, we are unable to ascertain whether there was any difference in therapies that might have influenced edema (e.g. corticosteroids). The inter-observer agreement for peritumoral edema was only fair, the weakest agreement of those MRI criteria identified as significant by multivariate analysis. This probably results from the subjective recording of edema by the investigators as previously reported (Dickinson et al., 2008; Kraft et al., 1997) in contrast to using an objective measurement. A measurement system has been developed for canine meningioma (Sturges et al., 2008), but it did not correlate with grade or type of meningioma and may not be easy to apply to gliomas.

While we confirmed that most gliomas are T1W-hypointense (Snyder et al., 2006; Young et al., 2011), our multivariate analyses appeared to indicate that astrocytomas constitute significantly more of the T1W-iso- or hyper-intense tumors, without any increase in GRE signal voids in astrocytomas (36%) over oligodendrogliomas (49%). It should be noted that the investigators were instructed to record the predominant T1W-signal; a largely hypo-intense tumor with a focus of hyper-intensity would have been recorded as hypo-intense. While iso- and hyper-intense astrocytomas and glioblastomas have been repeatedly reported in dogs (Kraft et al., 1997; Lipsitz et al., 2003; Snyder et al., 2006), our study are not

consistent with a comparison of T1W-hypo-intensity in astrocytoma and oligodendroglioma by Young (2011), indicating that our findings should be interpreted cautiously.

Human oligodendrogliomas are largely T1W-hypo-intense (Lee and Tassel, 1989), yet pilocytic astrocytomas are usually T1W-iso- to hyper-intense (Arai et al., 2006; Komotar et al., 2008), although no direct comparison of T1W-intensity has been reported. The reason why astrocytomas might be T1W-hyper-intense is unclear; iron and manganese levels in astrocytomas have not been well studied and lipids are not present histopathologically. Hepcidin (Hänninen et al., 2009), which functions in iron export, and frataxin (Kirches et al., 2011), which is involved in mitochondrial iron homeostasis, have been found to be reduced in tissues or cell lines of human astrocytomas, but the radiological implications of such aberrations have not been investigated.

One limitation of the current study is that most pathological diagnoses were made with surgical biopsies, which may underdiagnose the highest grade tumors. The hallmarks of glioblastoma include pleomorphism, glomeruloid vascular proliferations, and palisading of neoplastic cells around necrotic foci (Koestner et al., 1999). Biopsies that are not sufficiently extensive to characterize the degree of pleomorphism or miss areas of necrosis could lead to underdiagnosis of higher grade tumors as reported in humans (Dean et al., 1990).

Multiple statistically significant relationships were identified in our study, perhaps because 155 MRI interpretations were considered rather than 31 individual tumors. This methodology wherein each tumor is represented five times may advantageously decrease the significance of criteria displaying poor inter-observer agreement, but may also magnify the significance of individual outliers that are not representative of the general population. The case number was certainly inadequate to analyze each different subtype (for example comparing grade II astrocytomas and oligodendrogliomas) which might be the best way to investigate MRI criteria that are affected by both type and grade.

Conclusions

Gliomas that show no to mild contrast enhancement and no cystic structures and that occur superficial to the internal capsule, are more likely grade II tumors. Tumors that do not distort ventricles but show pronounced peritumoral edema are more likely to be astrocytomas than oligodendrogliomas. These findings can be applied once clinicians have made a diagnosis of likely intra-axial primary brain tumor based upon clinical and MRI criteria, but other neoplastic and non-neoplastic lesions should remain in the differential diagnosis.

Acknowledgments

The authors thank Matthew Hunt MD for assistance in obtaining surgical biopsies from some of the cases used in this study. We would also like to thank Dr. Annette Litster for reviewing the manuscript. Work was supported, in part, by American Cancer Society RSG-09-189-01-LIB (Ohlfest) and National Institute of Health R21 NS070955 (Ohlfest). Portions of this study were presented at the 2012 American College of Veterinary Internal Medicine Forum, New Orleans, LA.

References

Arai K, Sato N, Aoki J, Yagi A, Taketomi-Takahashi A, Mortia H, Koyama Y, Oba H, Ishiuchi S, Saito N, et al. MR signal of the solid portion of pilocytic astrocytoma on T2-weighted images: is it useful for differentiation from medulloblastoma? Neuroradiology. 2006; 48:233–7. [PubMed: 16550430]

Bentley, RT.; Ober, CP.; Pluhar, GE.; Packer, RA.; Litster, A.; Feeney, DA.; Ohlfest, JR. Comparison of magnetic resonance imaging features with histopathological type and grade of canine primary

intra-axial brain tumors. Proceedings of the 23rd Annual Symposium of the European Society of Veterinary Neurology; Cambridge, UK. 2010. p. 79

Bley CR, Sumova A, Roos M, Kaser-Hotz B. Irradiation of brain tumors in dogs with neurologic disease. Journal of Veterinary Internal Medicine. 2005; 19:849–854. [PubMed: 16355679]

Brearley MJ, Jeffrey ND, Phillips SM, Dennis R. Hypofractionated radiation therapy of brain masses in dogs: a retrospective analysis of survival of 83 cases (1991–1996). Journal of Veterinary Internal Medicine. 1999; 13:408–412. [PubMed: 10499721]

Cavaliere R, Lopes MBS, Schiff D. Low grade gliomas: an update on pathology and therapy. Lancet Neurology. 2005; 4:760–770. [PubMed: 16239183]

Cervera V, Mai W, Vite CH, Johnson V, Dayrell-Hart B, Seiler GS. Comparative magnetic resonance imaging findings between gliomas and presumed cerebrovascular accidents in dogs. Veterinary Radiology and Ultrasound. 2011; 52:33–40. [PubMed: 21322385]

Dean BL, Drayer BP, Bird CR, Flom RA, Hodak JA, Coons SW, Carey RG. Gliomas: classification with MR imaging. Radiology. 1990; 174:411–5. [PubMed: 2153310]

Dickinson PJ, Sturges BK, Higgins RJ, Roberts BN, Leutenegger CM, Bollen AW, LeCouteur RA. Vascular endothelial growth factor mRNA expression and peritumoral edema in canine primary central nervous system tumors. Veterinary Pathology. 2008; 45:131–9. [PubMed: 18424825]

Engelhard HH, Stelea A, Mundt A. Oligodendroglioma and anaplastic oligodendroglioma: clinical features, treatment and prognosis. Surgical Neurology. 2003; 60:443–456. [PubMed: 14572971]

Forbes JA, Chambless LB, Smith JG, Wushensky CA, Lebow RL, Alvarez J, Pearson MM. Use of T2 signal intensity of cerebellar neoplasms in pediatric patients to guide preoperative staging of the neuraxis. Journal of Neurosurgey Pediatrics. 2011; 7:165–174.

Giri DK, Aloisio F, Ajithdoss DK, Ambrus A, Lidbury JA, Hein HE, Porter BF. Giant cell glioblastoma in the cerebrum of a Pembroke Welsh Corgi. Journal of Comparative Pathology. 2011; 144:324–327. [PubMed: 21146179]

Hänninen MM, Haapasalo J, Haapasalo H, Fleming RE, Britton RS, Bacon BR, Parkkila S. Expression of iron-related genes in human brain and brain tumors. BMC Neuroscience. 2009; 10:36. [PubMed: 19386095]

Jenkinson MD, Du Plessis DG, Walker C, Smith TS. Advanced MRI in the management of adult gliomas. British Journal of Neurosurgery. 2007; 21:550–561. [PubMed: 18071982]

Kirches E, Andrae N, Hoefer A, Kehler B, Zarse K, Leverkus M, Keilhoff G, Schonfeld P, Schneider T, Wilisch-Neumann A, Mawrin C. Dual role of the mitochondrial protein frataxin in astrocytic tumors. Laboratory Investigation. 2011; 91:1766–1776. [PubMed: 21863062]

Koestner, A.; Bilzer, T.; Fatzer, R.; Summers, B.; Van Winkle, T. Histologic classification of tumors of the nervous system of domestic animals. 2. Washington, DC: Armed Forces Institute of Pathology; 1999.

Komotar R, Zacharia B, Sughrue M, Mocco J, Carson B, Tihan T, Otten M, Burger PC, Garvin JH, Khandji AG, Anderson RC. Magnetic resonance imaging characteristics of pilomyxoid astrocytoma. Neurological Research. 2008; 30:945–951. [PubMed: 18662499]

Kraft SL, Gavin PR, Leathers CW, Wendling LR, Frenier S, Dorn RV. Diffuse cerebral and leptomeningeal astrocytoma in dogs: MR features. Journal of Computer Assisted Tomography. 1990; 14:555–560. [PubMed: 2370354]

Kraft SL, Gavin PR, DeHaan C, Moore M, Wendling LR, Leathers CW. Retrospective review of 50 canine intracranial tumors evaluated by magnetic resonance imaging. Journal of Veterinary Internal Medicine. 1997; 11:218–225. [PubMed: 9298476]

Landis JR, Koch GG. The measurement of observer agreement for categorical data. Biometrics. 1977; 33:159–174. [PubMed: 843571]

Lee YY, Tassel PV. Intracranial oligodendrogliomas: imaging findings in 35 untreated cases. American Journal of Roentgenology. 1989; 152:361–369. [PubMed: 2783515]

Lipsitz D, Higgins RJ, Kortz GD, Dickinson PJ, Bollen AW, Naydan DK, LeCouteur RA. Glioblastoma multiforme: clinical findings, magnetic resonance imaging, and pathology in five dogs. Veterinary Pathology. 2003; 40:659–669. [PubMed: 14608019]

Louis DN, Ohgaki H, Wiestler OD, Cavenee WK, Burger PC, Jouvet A, Scheithauer BW, Kleihues P. The 2007 WHO classification of tumours of the central nervous system. Acta Neuropathologica. 2007; 114:97–109. [PubMed: 17618441]

MacKillop E, Thrall DE, Ranck RS, Linder KE, Munana KR. Imaging diagnosis-synchronous primary brain tumors in a dog. Veterinary Radiology and Ultrasound. 2007; 48:550–553. [PubMed: 18018727]

McConnell JF, Platt S, Smith KC. Magnetic resonance imaging findings of an intracranial medulloblastoma in a Polish Lowland Sheepdog. Veterinary Radiology and Ultrasound. 2004; 45:17–22. [PubMed: 15005356]

Polizopoulou ZS, Koutinas AF, Souftas VD, Kaldrymidou E, Kazakos G, Papadopoulos G. Diagnostic correlation of CT-MRI and histopathology in 10 dogs with brain neoplasms. Journal of Veterinary Medicine A, Physiology, Pathology, Clinical Medicine. 2004; 51:226–231.

Provenzale JM, Mukundan S, Barboriak DP. Diffusion-weighted and perfusion MR imaging for brain tumor characterization and assessment of treatment response. Radiology. 2006; 239:632–649. [PubMed: 16714455]

Rao PJ, Jyoti R, Mews PJ, Desmond P, Khurana VG. Preoperative magnetic resoance spectroscopy improves diagnostic accuracy in a series of neurosurgical dilemmas. British Journal of Neurosurgery. 2013 Epub ahead of print.

Ródenas S, Pumarola M, Gaitero L, Zamora A, Añor S. Magnetic resonance imaging findings in 40 dogs with histologically confirmed intracranial tumours. The Veterinary Journal. 2011; 187:85–91. [PubMed: 19914851]

Snyder JM, Shofer FS, Van Winkle TJ, Massicotte C. Canine intracranial primary neoplasia: 173 cases (1986–2003). Journal of Veterinary Internal Medicine. 2006; 20:669–675. [PubMed: 16734106]

Sturges BK, Dickinson PJ, Bollen AW, Koblik PD, Kass PH, Kortz GD, Vernau KM, Knipe MF, Lecouteur RA, Higgins RJ. Magnetic Resonance Imaging and Histological Classification of Intracranial Meningiomas in 112 Dogs. Journal of Veterinary Internal Medicine. 2008; 22:586–595. [PubMed: 18466258]

Watanabe M, Tanaka R, Takeda N. Magnetic resonance imaging and histopathology of cerebral gliomas. Neuroradiology. 1992; 34:463–469. [PubMed: 1436452]

Wolff CA, Holmes SP, Young BD, Chen AV, Kent M, Platt SR, Savage MY, Schatzberg SJ, Fosgate GT, Levine JM. Magnetic resonance imaging for the differentiation of neoplastic, inflammatory, and cerebrovascular brain disease in dogs. Journal of Veterinary Internal Medicine. 2012; 26:589–597. [PubMed: 22404482]

Young BD, Levine JM, Porter BF, Chen-Allen AV, Rossmeisl JH, Platt SR, Kent M, Fosgate GT, Schatzberg SJ. Magnetic resonance imaging features of intracranial astrocytomas and oligodendrogliomas in dogs. Veterinary Radiology and Ultrasound. 2011; 52:132–141. [PubMed: 21388463]

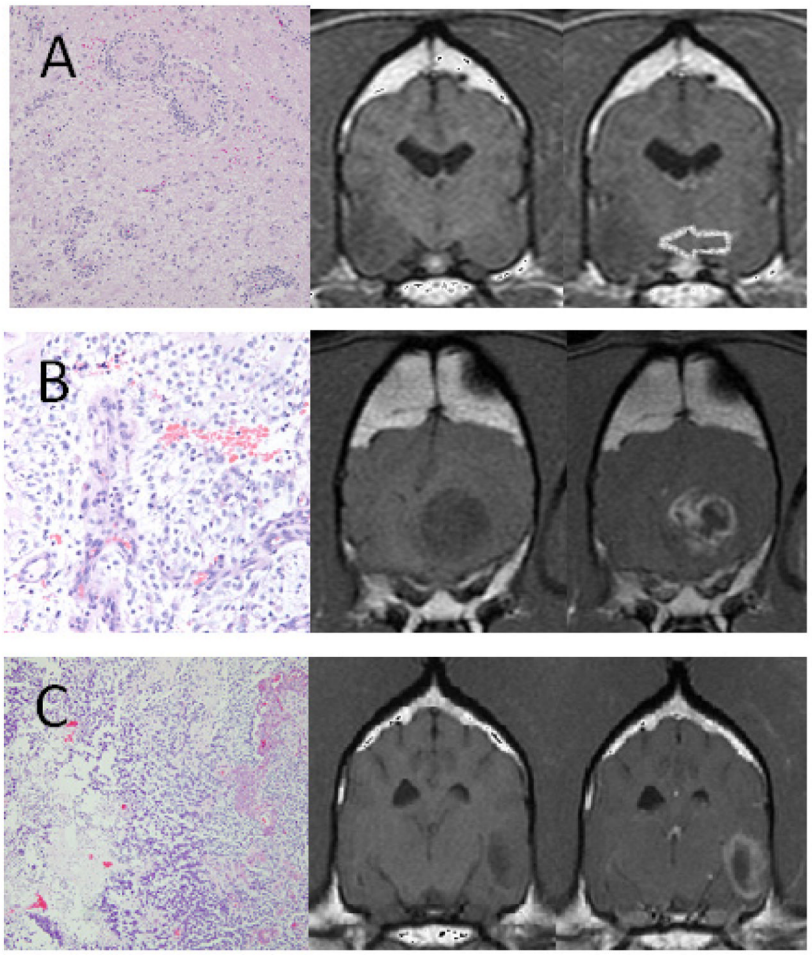

Fig 1.

Canine intracranial gliomas: Grade II (A - Astroctyoma), Grade III (B - Olidodendroglioma) and Grade IV (C - Glioblastoma). From left to right: Hematoxylin and eosin stained photomicrographs, T1W and T1W post-contrast transverse magnetic resonance images. The Grade II astrocytoma is non-enhancing and superficially located (arrow). Histopathologically, it displays no microvascular proliferation or necrosis. The Grade III oligodendroglioma is in a deeper location, contains multiple intra-tumoral fluid accumulations, and is severely enhancing in a ring-like pattern. Histopathologically, it is intermediate, displaying microvascular proliferation. The glioblastoma displays severe ring enhancement and a single cyst. Histopathologically, necrosis and cavitation, microvascular proliferation and profound pleomorphism are present.

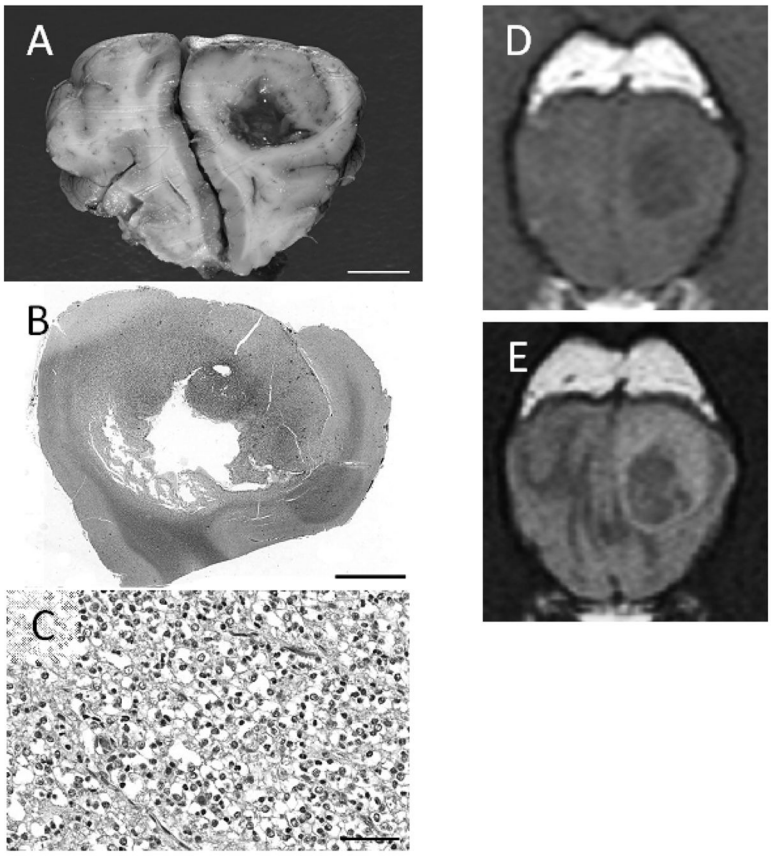

Fig 2.

Grade III canine oligodendroglioma, gross (A; bar = 1 cm), sub-gross Hematoxylin and eosin stained (B; bar = 5 mm), Hematoxylin and eosin stained photomicrograph (C; bar = 50 μm), with matching transverse T1W (D) and T2W fluid attention inversion recovery (E) magnetic resonance images. The lesion is T1-hypointense and peritumoral edema is not pronounced. Cystic cavitation is present.

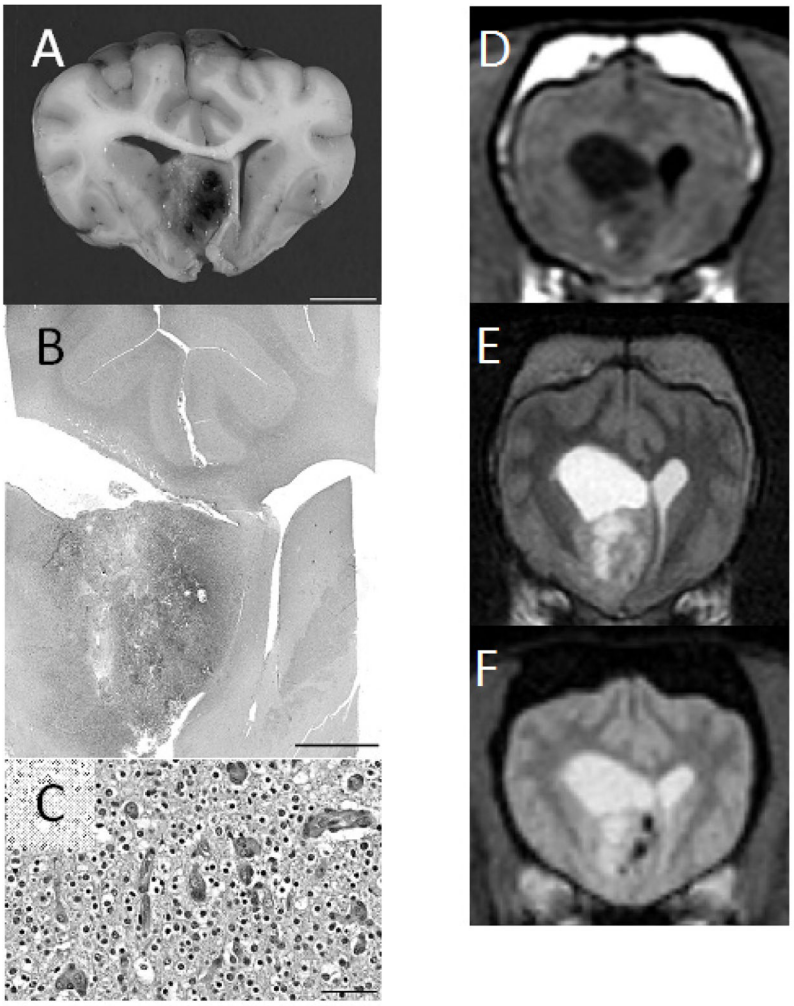

Fig 3.

Grade III canine oligodendroglioma, gross (A; bar = 1cm), sub-gross Hematoxylin and eosin stained (B; bar = 5 mm), Hematoxylin and eosin stained photomicrograph (C; bar = 50 μm), with matching T1W (D), T2W (E) and T2*-weighted gradient echo (F) transverse magnetic resonance images. There is notable ventricular distortion on magnetic resonance imaging (the lateral ventricles have collapsed post-mortem), minimal peritumoral edema, and the largest fraction of the tumor is T1W-hypointense. Multiple intratumoral fluid accumulations are present, as are gradient echo signal voids which coincide well with hemorrhagic regions seen pathologically.

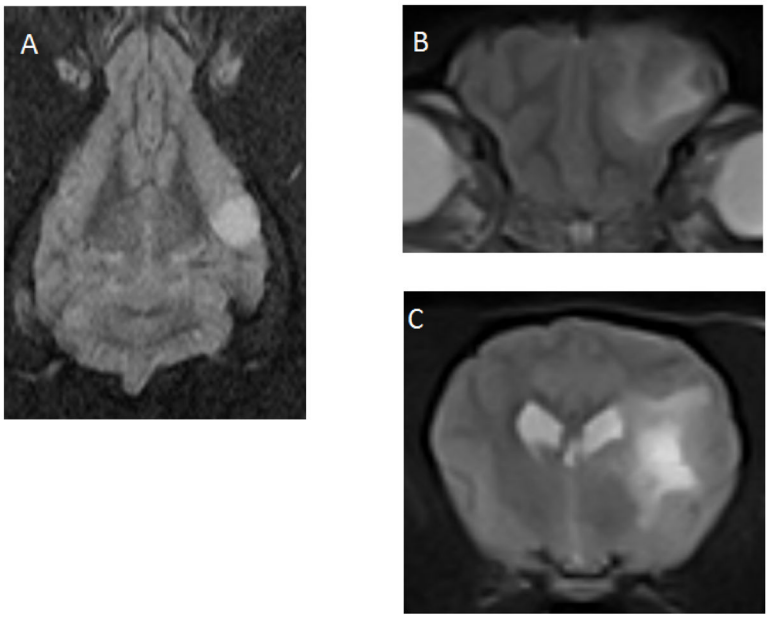

Fig 4.

Magnetic resonance T2W images of a canine oligodendroglioma (dorsal, A) and a canine astrocytoma (transverse, B and C). No peritumoral edema surrounds the oligodendroglioma. In contrast, the temporal astrocytoma (C) displays severe peritumoral edema, extending into the rostral aspect of the frontal lobe (B).

Table 1

Standardized grading scheme for magnetic resonance imaging (MRI) criteria used in the study.

MRI criteria	Descriptions used in this study
1. Margins	Poorly defined; smooth; irregular
2. Shape	Spherical; ovoid; elongate; amorphous; lobulated
3. Mass effect	None; mild; moderate; severe
4. Distortion of adjacent ventricle	None; mild; moderate; severe
5. Cystic structures	None; single cyst; multiple intra-tumoral fluid accumulations (ITFs)
6. T2-intensity	Hypointense; isointense; hyperintense
7. T2-homogeneity	Homogenous; heterogeneous
8. T1-intensity	Hypointense; isointense; hyperintense
9. T1-homogeneity	Homogenous; heterogenous
10. Peri-tumoral edema	None; mild; moderate; severe; extensive
11. Degree of contrast enhancement	None; mild; moderate; severe
12. Contrast enhancement pattern	None; focal; non-uniform; uniform (entire tumor); partial ring; complete ring
13. Gradient echo signal voids	None; single focus; multifocal; diffuse (majority of tumor)
14. Brain herniations	None; midline shift or falcine herniation; transtentorial; foramen magnum
15. Pattern of tumor growth	Focal; crosses midline; multifocal
16. Leptomeningeal involvement	Yes; no
17. Origin	Intra-axial; extra-axial
18. Tumor location	Freehand description

Table 2

Histological type and grade of the 31 canine intracranial gliomas. Tumors were graded using criteria previously described for human tumors (Louis et al., 2007) and applied to canine gliomas (Young et al., 2011).

Tumors	Grade II	Grade III	Grade IV	Total
Astrocytoma	7	5	5	17
Oligodendroglioma	2	12	NA	14
Total	9	17	5	31

NA, Not applicable

Table 3

Median inter-observer agreement (κ value) for magnetic resonance imaging (MRI) criteria used by five investigators in the interpretation of MRIs of 31 dogs with intracranial gliomas.

Agreement	Median κ value	MRI criteria
Excellent	0.81 – 1.00	Intra- vs. extra-axial origin (1.00); Location 4 (Caudal fossa; 1.00); Gradient echo signal voids (0.91); Location 2 (Parietal or adjacent corpus callosum, temporal; 0.87); T1W-intensity (0.83)
Good	0.61 – 0.80	Location 1 (Frontal or fronto-olfactory; 0.63)
Moderate	0.41 – 0.60	Degree of contrast enhancement (0.60); T2W-intensity (0.56); T2W-homogeneity (0.54); Contrast pattern (0.50); Herniations (0.50); Ventricular distortion (0.48); Location 3 (Thalamo-capsular; 0.47); Mass effect (0.44); Shape (0.44); Cystic structures (0.41)
Fair	0.21 – 0.40	Peri-tumoral edema (0.40); Tumor margins (0.39); Pattern of growth (0.32); T1W-homogeneity (0.28)
Poor	0.01 – 0.20	Leptomeningeal involvement (0.02)
Chance agreement	0.00	None

Table 4

Preliminary analysis of magnetic resonance imaging (MRI) criteria of 31 canine intracranial gliomas based on histological grade. Tumors were graded using criteria previously described for human tumors (Louis et al., 2007) and applied to canine gliomas (Young et al., 2011).

	Grade II tumors (*n*=9; 45 MRI observations)	**Grade III tumors (*n*=17; 85 MRI observations)**	**Grade IV tumors (*n*=5; 25 MRI observations)**	***P* (Grade II vs. Grades III and IV)**
Contrast enhancement criteria				
Contrast pattern (all patterns)	Various	Various	Various	0.0021*
No contrast enhancement	47%	22%	0%	0.0004*
Partial or complete ring enhancement	20%	51%	64%	0.0001*
Moderate or severe contrast enhancement	24%	46%	64%	0.0010*
MRI signal criteria				
Gradient echo signal voids (*n*=24)	17%	51%	62%	0.0007*
T2W-heterogeneity	42%	62%	75%	0.0049*
T1W-heterogeneity	47%	65%	56%	0.034
T1W-hypointensity	78%	94%	60%	0.94
T2W-hyperintensity	91%	98%	92%	0.16
Tumor characteristics				
Single cyst	13%	36%	28%	0.0046*
Location 3 (Diencephalic and internal capsule)	4%	19%	24%	0.015
Multiple intra-tumoral fluid accumulations	18%	34%	32%	0.039
Location 1 (Frontal or fronto-olfactory)	38%	61%	28%	0.075
Location 2 (Parietal or adjacent corpus callosum, temporal)	53%	36%	36%	0.055
Peri-tumoral edema (moderate to extensive)	24%	29%	52%	0.13
Location 4 (Caudal fossa)	7%	0%	12%	0.25
Spherical or ovoid shape	56%	58%	80%	0.37
Pattern of growth (focal, crosses midline, multifocal)	80%, 13%, 7%	75%, 16%, 8%	80%, 20%, 0%	0.54
Regular margins	58%	53%	64%	0.79
Mass effect				
Distortion of ventricles	40%	84%	68%	0.0073*
Falcine herniation or midline shift	29%	51%	24%	0.068
Mass effect (none, mild, mod, sev)	9%, 64%, 18%, 9%	5%, 39%, 36%, 20%	16%, 68%, 16%, 0%	0.016
Foramen magnum herniation	0%	6%	0%	0.14
Transtentorial herniation	11%	11%	0%	0.55

* $P < 0.01$.

Each MRI was interpreted by five independent investigators resulting in 155 MRI observations from the 31 gliomas. Leptomeningeal involvement (poor agreement) and intra-axial origin (ubiquitous presence in every grade) were excluded from the analysis.

Mod, moderate; Sev, severe.

Table 5

Preliminary analysis of magnetic resonance imaging (MRI) criteria of 31 canine intracranial gliomas according to histologic tumor type.

	Astrocytomas (*n*=17; 85 MRI observations)	**Oligodendrogliomas (*n*=14; 70 MRI observations)**	***P***
Contrast enhancement criteria			
Contrast pattern (all patterns)	Various	Various	0.63
No contrast enhancement	21%	31%	0.10
Partial or complete ring enhancement	41%	47%	0.46
Moderate or severe contrast enhancement	42%	43%	0.95
MRI signal criteria			
T1W-hypointensity	76%	93%	0.0064*
Gradient echo signal voids (n=23)	36%	49%	0.12
T1W-heterogeneity	64%	51%	0.13
T2W-hyperintensity	93%	97%	0.22
T2W-heterogeneity	56%	57%	0.93
Tumor characteristics			
Peri-tumoral edema (moderate, severe or extensive)	40%	21%	0.012
Location 4 (Caudal fossa)	14%	7%	0.024
Pattern of growth (focal, crosses midline, multifocal/diffuse)	76%, 20%, 4%	79%, 11%, 10%	0.044
Spherical or ovoid shape	55%	67%	0.11
Location 3 (Diencephalic and internal capsule)	12%	20%	0.16
Location 2 (Parietal or adjacent corpus callosum, temporal)	38%	46%	0.32
Location 1 (Frontal or fronto-olfactory)	52%	46%	0.46
Multiple intra-tumoral fluid accumulations	31%	27%	0.62
Single cyst	26%	29%	0.71
Regular margins	55%	57%	0.82
Mass effect			
Distortion of ventricles	66%	84%	0.0068*
Foramen magnum herniation	0%	7%	0.011
Mass effect (none, mild, moderate, severe)	8%, 59%, 22%, 11%	7%, 41%, 34%, 17%	0.047
Falcine herniation or midline shift	36%	44%	0.32
Transtentorial herniation	9%	9%	0.85

* $P < 0.01$.

Each MRI was interpreted by five independent investigators resulting in 155 MRI observations from the 31 tumors. Leptomeningeal involvement (poor agreement) and intra-axial origin (ubiquitous presence in every grade) were excluded from the analysis.